13

Surface modification of polymer films with low-energy electron beam (8.5 keV)

© V.I. Pavlenko, S.N. Domarev, O.D. Edamenko, V.V. Kashibadze, A.Yu. Ruchii

Belgorod State Technology University named after V.G. Shukhov,
308010 Belgorod, Russia
e-mail: domarev542@gmail.com

Received February 9, 2024
Revised June 24, 2024
Accepted July 11, 2024

The physical and mechanical properties and structure of polyimide (PI), polyethylene terephthalate (PET) and polytetrafluoroethylene (PTFE) polymer films treated with electron beam with the energy of 8.5 keV have been investigated. It is shown that the optical characteristics of the films change depending on the electron fluence, and the degree of manifestation of the observed effects (5–8% decrease of light transmittance of PTFE films and increase of light transmittance of PI and PET films) depends on this parameter. It has been discovered that the reason for changes in the optical properties of polymer films is the occurrence of defects in the structure of samples, primarily associated with thermal degradation processes. It is also shown that with the help of low-energy electron beam it is possible to change the surface free energy, the increase of the polar part of which is connected with the increase of the number of polar groupings near the surface.

Keywords: polymer films, polyimide, polyethylene terephthalate, fluoroplast, surface, irradiation, electron beam, fluence,surface free energy.

DOI: 10.61011/TP.2024.10.59368.34-24

Introduction

Controlled adjustment of properties of materials through modification of their surface is used widely in modern industry. The modification method involves altering the chemical structure and physical characteristics of the surface of a polymer material with the aim of improving such characteristics as adhesion, wettability, and biocompatibility [1,2]. One way to modify polymer materials is electron-beam processing, which allows one to alter the surface layer of materials to a certain specific depth without rearranging the structure of underlying layers.

A considerable number of papers focused on low-energy electron-beam modification of the surface of polymer materials have already been published [1,3]. For example, surface modification of a polyethylene terephthalate (PET) film by an electron beam with an energy of 75 keV at electron fluences ranging from $1.3 \cdot 10^{-19}$ to $6.6 \cdot 10^{-19}$ cm^{-2} was discussed in [1]. The authors noted that the most profound changes were observed for the surface free energy (SFE) calculated by the Owens–Wendt–Rabel–Kaelble (OWRK) method from the measured contact angles of wetting the surface with liquid in the diiodomethane–water and glycerol–water systems. The correlation of these changes with the electron fluence is significant only for the polar SFE part; the observed variation of the disperse SFE part at fluences above $1.3 \cdot 10^{-19}$ cm^{-2} lie within the confidence intervals of the estimate of the parameter in question. The authors did also evaluate surface roughness using atomic force microscopy. The presented results demonstrate unambiguously that this parameter increases with electron fluence; according to the surface topology data, the change in surface roughness is associated primarily with the emergence of protrusions, which increase in number with increasing fluence.

The authors of [4] used a slightly different approach. The results of modification of polymer films made of polyimide (PI), polytetrafluoroethylene (PTFE), and other fluorinated polymers by low-energy electron beams were examined using the electron spin resonance (ESR) and thermogravimetric analysis (TGA) methods. These studies were conducted within the 40–110 keV energy range. According to the reported data, free radicals, which manifest themselves in ESP spectra, are produced in the bulk of materials. Notably, an increase in electron beam energy leads to an increase in signal intensity, which is directly related to the yield of free radicals. The TGA study of polymers processed with an electron beam indicates a change in the dynamics of polymer mass loss with an increase in irradiation dose: the loss rate decreases after electron-beam treatment. In addition to the above findings, the authors noted a significant improvement in wettability of polymers; however, the presented data provide only a qualitative estimate, precluding one from comparing them with the data from other published studies.

Since electron-beam irradiation is a type of radiation treatment performed for the purpose of improving and imparting new properties to materials, one needs to take into account the aspect of radiation resistance of polymers. These issues were discussed in a number of papers [5,6]. The authors noted that when polymers are irradiated with an electron beam, a number of effects other than surface

modification arise, and some of these effects associated with modification of the chemical structure are undesirable.

Changes in material properties under electron-beam irradiation and defects produced in the course of such treatment were also examined in [3,7–9], but the majority of these studies are focused on fairly high (30−300 keV) beam energies, which correspond to penetration powers that are ill-suited for surface modification of materials. For example, the damage to solid polymer materials subjected to electron irradiation with an energy of 200−300 keV was considered in [9]; in the experiment, samples of polymethyl methacrylate (PMMA) and plastic based on epoxy-diane resin were used. The key regions of material destruction located at different distances from the surface of the sample were revealed clearly. These data are taken into account in the present study when the influence of an electron beam on the material is modeled.

Thus, although the issue of controlled surface modification is fairly well-investigated in general, the resulting damage to polymer materials is rarely mentioned in published papers, and those studies that do pay attention to such damage deal with high-energy electrons (up to 1 GeV) [10].

The aim of the present study is to identify and examine the surface modification, structural damage, and changes in the optical characteristics resulting from irradiation of polymer films with a low-energy electron beam (8.5 keV) at different ($1.37 \cdot 10^{-17}$–$4.11 \cdot 10^{-17}$ cm^{-2}) fluences. The observed variations are identified and characterized using the methods of photography and processing of the obtained images, IR spectroscopy, and UV−visible−near-IR spectroscopy; changes in the surface structure of polymer films are examined via OWRK measurements of the surface free energy.

1. Methods and materials

1.1. Materials

Polyimide (DuPont Kapton film), PET (DuPont Mylar PET film), and polytetrafluoroethylene (DuPont Teflon PTFE film) polymer films with a thickness of 20 μm were used to prepare the samples. Square-shaped samples with a side length of 20 mm were cut from these films. The obtained samples were positioned on a quartz glass substrate and secured with UHV-compatible adhesive tape (UHV Kapton® Tape).

1.2. Setup for film irradiation

Films were irradiated at the electron-beam setup („Vakuumnye sistemy i elektronika“, Russia) in the Laboratory of Space Material Research at the Belgorod State Technology University named after V.G. Shukhov. The diagram of the experimental setup is shown in Fig. 1.

The constancy of beam parameters, namely the accelerating voltage and current, was monitored via the specialized EGun software („Vakuumnye sistemy i elektronika“, Novosibirsk) that was used to control the electron-beam setup. The setup was operated in the automatic beam current adjustment mode to maintain it at a level of 70 μA throughout the entire experiment.

Figure 1. Setup for irradiating materials with an electron beam (the central part is a cutaway view): *1* — LaB6 electron thermal emitter; *2* — accelerating anode (8.5 kV); *3* — focusing coils; *4* — longitudinal and transverse bias coils; and *5* — material sample.

1.3. IR spectrometry

Fourier-transform IR spectra of pristine and irradiated films were obtained using an IR spectrophotometer (Bruker); measurements were carried out within the 4000–400 cm^{-1} interval. To reduce the impact of atmospheric air on the samples during transportation, irradiated films were kept in sealed bags from which most of the air was evacuated. Spectra were recorded immediately after the samples were removed from the setup.

1.4. Optical spectrometry

UV-visible spectra of pristine and irradiated films were obtained using a Leki SS1207 (Finland) spectrophotometer in the transmission (Tr) mode within the wavelength range from 360 to 1000 nm with a step of 20 nm. The samples were secured in a four-position film holder; the outer position was left vacant for calibration (Tr — 100%).

1.5. Photography

Photographic recording of cathodoluminescence of polymer films exposed to an electron beam and the resulting damage was performed using a Sony Alpha α58 (China) CMOS (complementary metal-oxide-semiconductor) camera with a SAM II 18−55 mm (Sony, China) lens. This

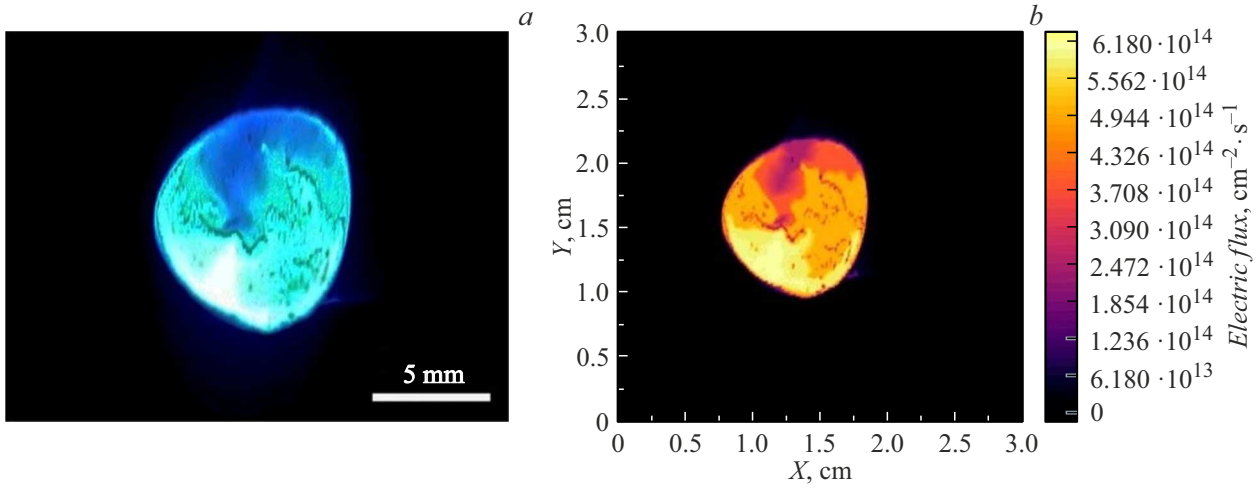

Figure 2. Spatial distribution of the particle flux density: *a* — initial photographic recording data; *b* — plotted spatial distribution map.

recording was done manually with the same parameters for all samples. Cathodoluminescence of the films was photographed with a long exposure (15 s) through the viewing window of the sample irradiation chamber of the electron-beam setup.

1.6. SFE measurement

To calculate the SFE, the contact angle was measured using the sessile drop method with a DSA 30 (Kruss, Germany) instrument. Each of the presented results was averaged over five parallel measurements for each of the samples obtained under different irradiation conditions. The disperse and polar parts of the surface free energy were calculated by the OWRK method using the results of measurements of the contact angle of wetting the sample surface with polar and non-polar solvents (deionized water and diiodomethane, respectively).

2. Results and discussion

2.1. Refinement of parameters of the electron beam

The key figures characterizing the beam were calculated in order to refine its parameters. The results of photographic recording of cathodoluminescence of the phosphor on the plate were used (Fig. 2, *a*) in calculations to determine the spatial distribution of the particle flux density. The total number of particles (N) was calculated as

$$N = \frac{I \cdot t}{q_e},$$

where I is the beam current strength, t is the film irradiation time, and q_e is the charge. The time-averaged value of beam current ($70\,\mu$A) was assumed to be the current strength. The charge was taken equal to the charge of a single electron ($1.60217663 \cdot 10^{-19}$ C), and the irradiation time of films was 1 s, since the average particle flux density for a unit time interval was considered. With these parameters, the total number of particles is $4.566 \cdot 10^{14}$. This value is needed to determine the electron flux density through the sample material and to calculate the time-averaged particle fluence.

Photographic images of the beam were then processed in ImageJ to plot a map of the distribution of the particle flux density of the beam in a plane perpendicular to it. The output was a three-dimensional matrix with each pixel corresponding to a coordinate on the plane, and the pixel intensity was used in further calculations.

Since the beam is, to a certain extent, monoenergetic (8.5 keV), the relative beam glow intensity (represented by shades of gray 255...0) was associated with the electron flux density; the functional dependence between these quantities was assumed to be linear in the discussed experiment.

Operations were performed on the obtained matrix to calculate the particle flux density at each point of the beam. It was assumed in calculations that all previously calculated particles ($4.566 \cdot 10^{14}$) fall within the geometric region of the beam. The resulting spatial distribution of flux characteristics of the beam is shown in Fig. 2.

The data presented in Fig. 2, *b* reveal an uneven distribution of the particle flux density, which is attributable to nonuniform heating of the lanthanum hexaboride pellet and to the specifics of operation of electron optics. However, it is worth noting that the particle flux density values are spread within one order of magnitude, and the difference is no greater than three-fold within the majority of the beam area.

2.2. Modeling of the propagation of electrons through polymers

Computer Monte Carlo simulation was performed in CASINO v. 2.481 [11] to study the interaction of the electron beam with an energy of 8.5 keV with polymer films. The

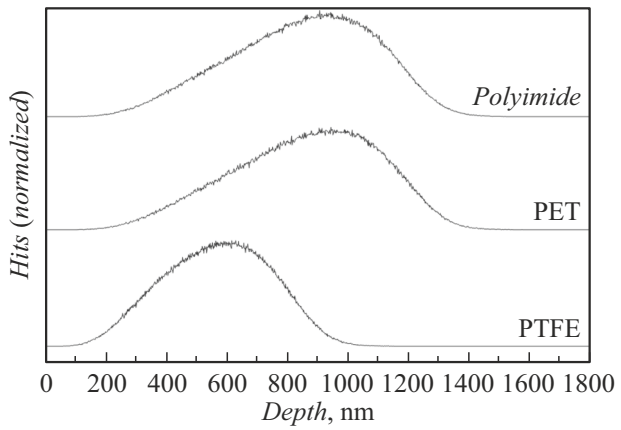

Figure 3. Models of the depth of penetration of electrons with an energy of 8.5 keV into the material.

mentioned program uses tabulated elastic interaction cross sections (Mott) and experimentally determined deceleration forces to calculate the trajectories of electrons in matter [12]. The values obtained in calculations in CASINO v. 2.481 provide an opportunity to determine the crucial parameters of the problem, including the penetration depth of electrons, the material volume exposed to irradiation, and the distribution of the energy density transferred to the material from the electron beam.

Figure 3 presents the calculated depths of electron penetration into the material (polymer) at an electron beam energy of 8.5 keV. The depth at which the maximum number of electrons was recorded in the examined material samples is 610 nm for polytetrafluoroethylene and 940 nm for PI and PET. At greater depths, the number of detected particles decreased sharply. The results of modeling suggest that electrons lose all their energy and are stopped completely at a depth of 1094 nm in polytetrafluoroethylene and 1542 nm in PI and PET.

The propagation of primary electrons through the material is accompanied by their scattering and gradual loss of energy [11], which is calculated by the program (Fig. 3). In calculation, the material is divided into a certain number (specified in the program settings) of unit cells, and the volume is calculated automatically based on the maximum depth of electron penetration into the material.

One may divide the energy calculated by the program (keV) by the unit cell volume (nm^3) and determine the energy density ($J \cdot m^{-3}$ in SI units) distribution. The obtained value is valid for the number of electrons simulated by the program; if we additionally divide the energy density by the number of electrons, the resulting value ($J \cdot m^{-3} \cdot electron^{-1}$) will characterize the energy transferred to the sample material by a single electron propagating through it and provide an opportunity to calculate the transferred energy at points with different particle fluxes (Fig. 4).

2.3. Cathodoluminescence under electron irradiation and damage to films

Cathodoluminescence, which manifests itself in the emission of visible light quanta, is one of the phenomena observed when materials are irradiated with an electron beam. It is known that most polymer materials are, to a certain extent, prone to cathodoluminescence, and the recorded spectrum is sufficiently characteristic to identify polymers when examined via scanning electron microscopy [13]. The approximation of film glow colors in the CIE 1931 XY color space is (0.279, 0.321) for the PET film sample, (0.295, 0.300) for the PI film, and (0.419, 0.395) for the PTFE film.

Figure 5 illustrates the cathodoluminescence of samples observed in the experiment. Photographs were taken with identical settings; taking this into account, one may note a significant difference in the glow intensity of films. Specifically, the polytetrafluoroethylene film has the highest intensity of glow, which could be observed with the naked eye. The glow of PET is characterized by a lower intensity, but it is still significantly more intense than the PI film glow. The difference in intensity may be attributed to the difference in structures of the polymer monomer unit, which is found even in polymers of the same class [14].

The issue of the nature of cathodoluminescence of various polymers remains largely open [15]. One of the proposed mechanisms is the $\pi^* \rightarrow \pi$ transition in double (C=C) bonds, which are prominent in PI and PET and also form in polytetrafluoroethylene under irradiation [14]. A significant contribution of this transition is the most likely cause of the characteristic yellow glow of PTFE, since its energy is close to ~ 2.2 eV.

The glow of PET and PI samples in cathodoluminescence experiments is bluish in color, which may be attributed to the contribution of the C=O radiative transition characterized in [14]. The energy associated with this transition is ~ 2.4 eV.

The damage to irradiated films is also seen in Fig. 5. A significant degree of correlation between the nature of damage to the samples and the obtained spatial distribution of the particle flux density (Fig. 4) is worth noting. The presented photographic image also reveals the varying degrees of damage to the samples exposed to electron irradiation. Specifically, PI and PET samples have suffered the most severe damage, while the damage to the polytetrafluoroethylene sample becomes visible only after digital contrast enhancement.

According to the simulated data, thermal destruction of the polymer material, which manifests itself in darkening of the sample at points of local temperature rise, is one of the possible mechanisms behind the observed damage. The prerequisite for this is that a significant part of the total electron beam energy is dissipated in the surface (~ 400 nm) material layer, and one of the consequences is the dependence of the degree of sample darkening on irradiation dose. A similar kind of damage has been observed earlier in experiments on polymer irradiation

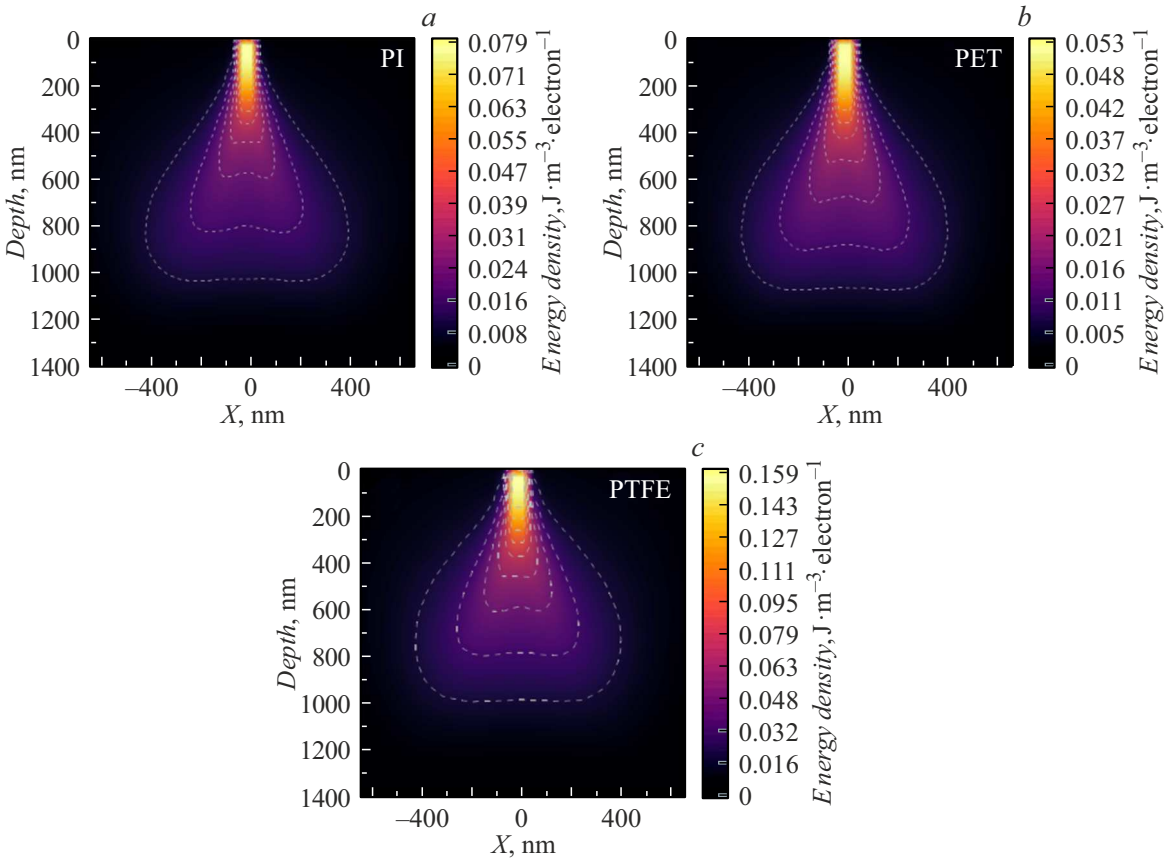

Figure 4. Spatial distribution of the beam energy absorbed by the material: *a* — PI film, *b* — PET film, and *c* — PTFE film.

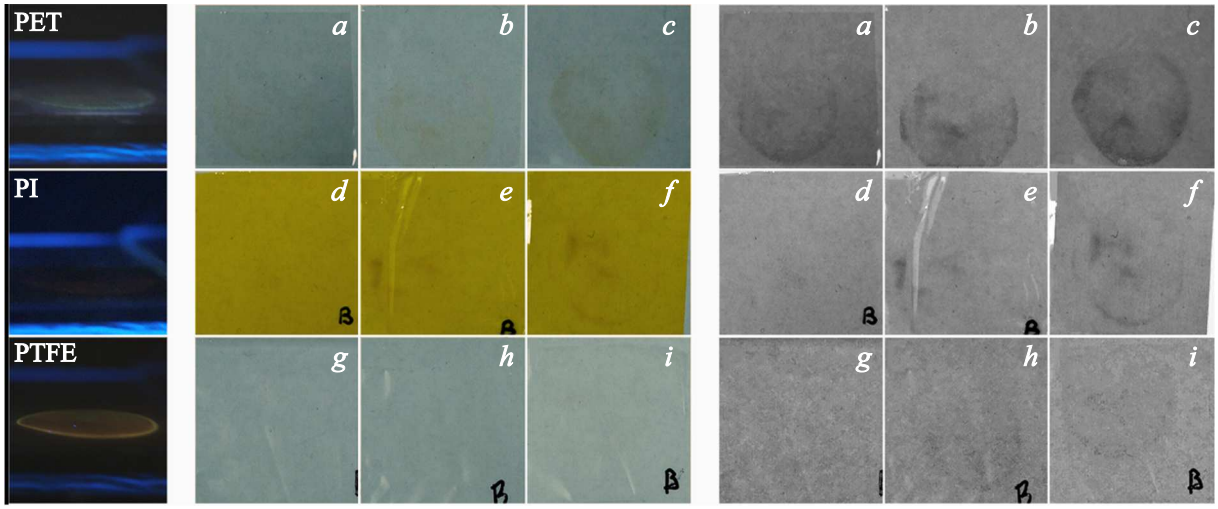

Figure 5. Photographic recording of cathodoluminescence processes and damage to films in normal (middle column) and high-contrast (rightmost column) modes: *a*–*c* — PI film, *d*–*f* — PET film, and *g*–*i* — PTFE film.

with electron beams with energies significantly higher than 8.5 keV [1,3,7,8].

2.4. IR spectra of films

The nature of chemical bonds in polymers may be investigated by characterizing the vibrational modes revealed by IR spectroscopy. Figure 6 shows the IR spectra of unirradiated and electron-irradiated samples. The fluence through the surface of the irradiated sample regions is indicated above the curves.

The absorption band with the strongest intensity in the spectra of PI samples (Fig. 6, *a*) is the one at 1750 cm^{-1}, which corresponds to asymmetric stretching vibrations (ν_{as})

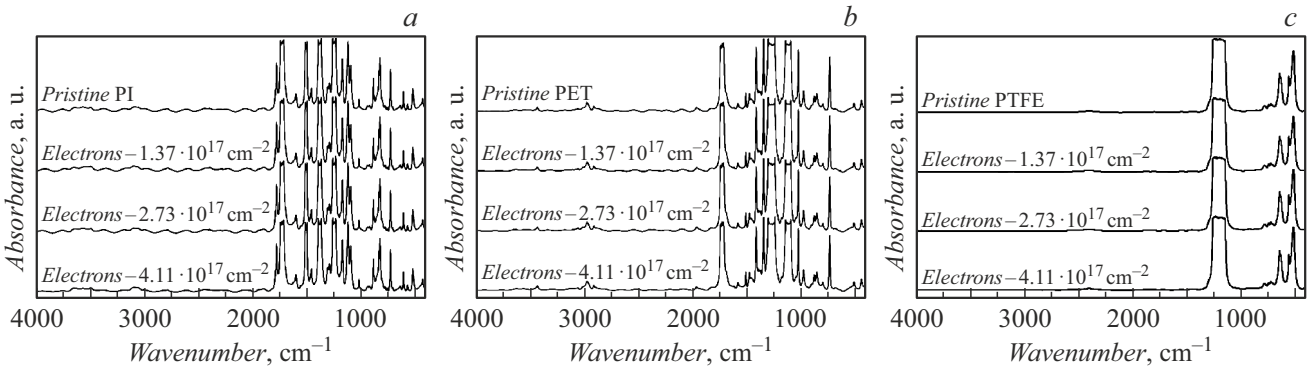

Figure 6. IR spectra of unirradiated and electron-irradiated samples of PI (*a*), PET (*b*), and PTFE (*c*).

of C=O bonds in imides; the adjacent peak of a slightly lower intensity at 1740 cm^{-1} corresponds to symmetric stretching vibrations (ν_s) of the same bonds. Peaks at 1500 cm^{-1} (skeletal stretching vibrations (ν) vibrations of the C−C benzene ring bond) and at 1320 cm^{-1} (stretching vibrations (ν) of the C−O bond) are also observed. The peak at 1250 cm^{-1}, which is attributed to deformation in-plane vibrations (δ) of the C−H benzene ring bond, and the peak at 1090 cm^{-1} corresponding to deformation vibrations (δ) of the C−C bond are fairly intense too [3,7,8].

IR spectra of PET film samples were obtained in a similar manner (Fig. 6, *b*). The intense absorption band at 1750 cm^{-1}, which corresponds to ν vibrations of the C=O bond, is also prominent in these spectra. The peak at 1320 cm^{-1}, which represents ν vibrations of the C−O bond, the absorption band at 1250 cm^{-1} corresponding to δ vibrations of the C−H benzene ring bond, and the peak at 1090 cm^{-1} corresponding to δ vibrations of the C−C bond are observed as well. The peak at 1500 cm^{-1} representing skeletal ν vibrations of the C−C benzene ring bond is significantly less intense, since the number of benzene rings in the polymer structure is lower [1].

The monomer unit of PET features a benzene ring and most of the bonds found in the structure of polyimide; this makes the spectra of polymers quite similar.

The obtained IR spectra of the PTFE film (Fig. 6, *c*) contain a significantly smaller number of peaks, which is attributable to a simpler linear structure of the polymer and the presence of just two bonds: C−C and C−F. The first one does not feature a dipole moment and, consequently, has very low activity with respect to IR radiation and is not represented in the IR spectra. The C−F bond has an absorption band in the range from 1250 to 1125 cm^{-1}, which corresponds to ν vibrations. The presence of peaks at 642, 631, 558, and 514 cm^{-1}, which represent δ vibrations of the C−F bond, is also noted [1,8,16].

Despite the change in macrostructure of polymer films that is seen clearly in the photographic images of samples, the spectra of all films demonstrated only a slight change in the intensity of certain absorption bands after irradiation. This is likely attributable to the fact that the observed film

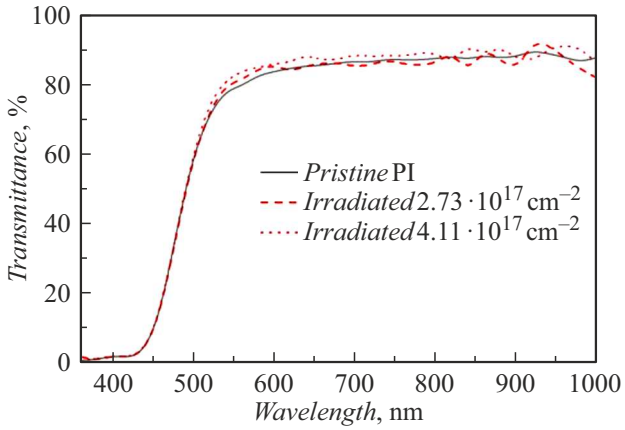

Figure 7. UV-visible spectra of the PI film at different fluences.

defects (darkening) form as a result of rupture of molecular chains in films, which involves the formation of free radicals, and subsequent reactions of free radicals with air molecules (a phenomenon also known as „healing“ of polymers in air after irradiation). Similar phenomena have already been noted in studies where the effect of bombardment of polymer PI [3,7], polytetrafluoroethylene [8], and PET [1] films with a monoenergetic electron flux was examined.

2.5. Transmission spectra of films in the UV-visible range

Certain optical parameters of the samples were modified after irradiation; a change in light transmittance in the UV-visible-near IR range (360−1000 nm) was noted for all three samples. Specifically, the light transmittance of PI (Fig. 7) within the 500−650 nm range increased slightly ($\sim$ 5%) with an increase in radiation dose absorbed by the sample. Since the changes within the 650−1000 nm range are irregular in nature, they cannot be characterized in any way. The absorption band associated with the $\pi \rightarrow \pi^*$ transition in double bonds (380−500 nm) also remains unchanged and, in general, characteristic of PI obtained

Calculated surface free energy for polymer film samples

Sample		γS, mN/m	γS_d, mN/m	γS_p, mN/m
PI film	Unirradiated	41.14 ± 0.99	40.39 ± 0.74	0.75 ± 0.25
	Irradiated	38.16 ± 3.34	36.59 ± 1.68	1.56 ± 1.66
PET film	Unirradiated	43.88 ± 2.38	42.06 ± 1.61	1.82 ± 0.77
	Irradiated	38.41 ± 1.60	34.46 ± 1.10	3.95 ± 0.50
PTFE	Unirradiated	23.04 ± 2.73	22.57 ± 1.50	0.47 ± 1.24
	Irradiated	34.55 ± 6.85	31.28 ± 4.50	3.27 ± 2.35

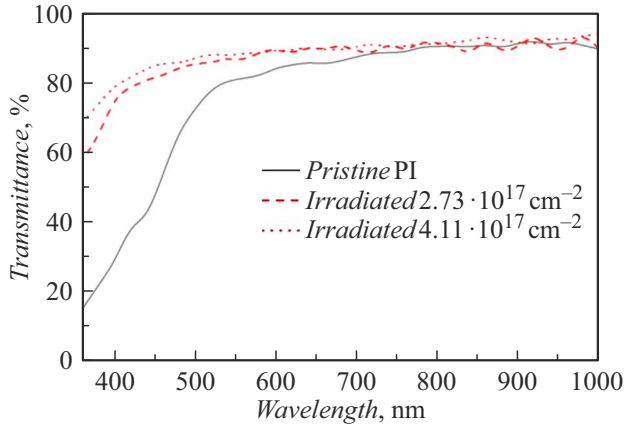

Figure 8. UV-visible spectra of the PET film at different fluences.

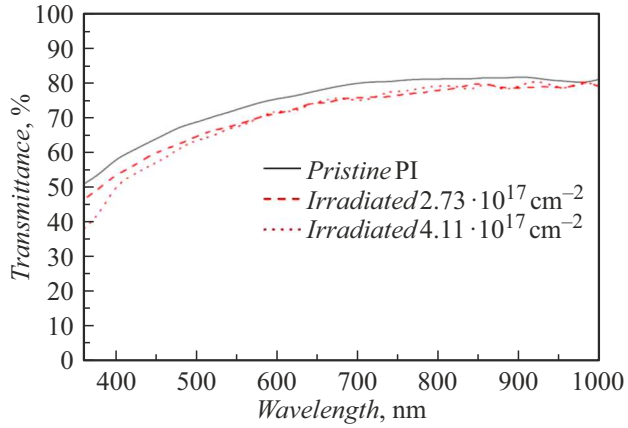

Figure 9. UV-visible spectra of the PTFE film at different fluences.

by polycondensation of pyromellitic dianhydride and 4, 4′-oxydiphenylamine [17].

The light transmittance of the PET film (Fig. 8) changes more profoundly after irradiation. Specifically, significant attenuation of the luminous flux by the samples in the 380–500 nm region, which corresponds to the absorption band associated with the $\pi \rightarrow \pi^*$ transition in double bonds that was examined earlier for the PI film, is observed at a fluence of $4.11 \cdot 10^{17}\,\mathrm{cm}^{-2}$. It is also noteworthy that the irradiated spot takes on a yellowish tint in the region of increased fluence. The change in film color is probably attributable to the formation of a larger number of double bonds, which have the capacity to absorb visible light within a certain wavelength range due to $\pi \rightarrow \pi^*$ transitions. A similar process is observed in the PI film: its color is the result of absorption in a number of transitions and is manifested as an „absorption edge“ at wavelengths below 500 nm [18] in the spectra.

No significant changes in light transmittance of the sample were observed after irradiation of the polytetrafluoroethylene film (Fig. 9). The light transmittance decreased by 5% within the 600–1000 nm range for samples irradiated with an electron fluence of $2.73 \cdot 10^{17}\,\mathrm{cm}^{-2}$ and $4.11 \cdot 10^{14}\,\mathrm{cm}^{-2}$. A reduction by another 5% was noted within the 360–600 nm range for the sample irradiated with a fluence of $4.11 \cdot 10^{14}\,\mathrm{cm}^{-2}$. This provides indirect evidence of disruption of molecular structures of polymer chains, which may occur as a result of production of free radicals [14].

All the examined effects may be divided into two groups: the distinguishing feature of the first one is „darkening“ within the entire UV-visible range, and the second group is characterized by emergence of spectral characteristics. Thus, the first effect is manifested in a nearly uniform reduction in light transmittance observed in polytetrafluoroethylene film samples. The second effect is the emergence of an „absorption edge“, which is similar to the one in PI, in PET film samples.

2.6. Investigation of the variation of surface free energy

The results of calculation of the surface free energy of irradiated polymer films by the OWRK method are presented in the table. Pristine polymer film samples and those irradiated with a fluence of $4.11 \cdot 10^{14}\,\mathrm{cm}^{-2}$ were used in this study.

The polar part of the surface free energy increases for all films after irradiation with electrons. This is associated with the polymer surface modification and the formation of

hydrophilic groups [1,19]. Notably, the surface free energy (γS) of the irradiated PI and PET film samples remains virtually unchanged, and the increase in polar (γS_p) SFE part is largely compensated by a reduction in disperse part (γS_d), which accounts for the hydrophobic properties of the material. This provides indirect evidence that the emerging changes are due to the rearrangement of the polymer surface structure, since the balance of disperse and polar parts shifts while the total SFE remains at the same level.

A significant change in surface free energy is observed for the polytetrafluoroethylene film, which suggests that the changes are external in nature. It is most likely that hydrophilic groups emerge during „healing“ of the polymer in air. This assumption is confirmed by the observations reported in [4]. In turn, the observed variation of the disperse part correlates well with the changes in contact angle of wetting of films with water that were observed in [19] with an increase in irradiation dose.

Conclusion

Experimental studies have demonstrated that an electron beam induces modification of the surface of polymer films. This is verified directly by an increase in hydrophilicity of the surface of polymer films as a result of electron irradiation. Specifically, γS_p is 1.56 ± 1.66 mN/m for PI film samples, 3.95 ± 0.50 mN/m for PET samples, and 3.27 ± 2.35 mN/m for polytetrafluoroethylene ones. This modification is the result of a change in the chemical structure of the surface layer of samples caused by the emergence of polar groupings.

In addition to surface modification, violation of structural integrity of the films, which is manifested in a change in their optical properties and in the emergence of visible defects (darkening), is observed. The change in optical properties of polytetrafluoroethylene films consists in a uniform 5% reduction of light transmittance throughout the entire UV-visible spectral range; in PET samples, the light transmittance decreases almost linearly at wavelengths below 500 nm.

Cathodoluminescence of films is also induced under irradiation with an electron beam. This effect is caused by radiative transitions in polymer bonds with different energies that shape the spectral characteristics of radiation and, consequently, impart characteristic colors to the observed glow, which are approximated in the CIE 1931 XY color space as (0.279, 0.321) for the PET film sample, (0.295, 0.300) for PI, and (0.419, 0.395) for polytetrafluoroethylene. This phenomenon has potential to be used for characterization of polymer compounds examined by scanning electron microscopy.

Funding

This study was supported by grant No. 19-79-10064 (renewal) from the Russian Science Foundation, https://rscf.ru/project/19-79-10064/. Equipment provided by the High-Technology Center of the Belgorod State Technology University named after V.G. Shukhov was used in experiments.

Conflict of interest

The authors declare that they have no conflict of interest.

References

[1] A. El-Saftawy, A. Elfalaky, M. Ragheb, S. Zakhary. Rad. Phys. Chem., **102**, 96 (2014). DOI: 10.1016/j.radphyschem.2014.04.025
[2] I.P. Ershov, L.A. Zenitova, F.R. Sagitova. Construction Mater. Products, **6** (4), 5 (2023). DOI: 10.58224/2618-7183-2023-6-4-5-14
[3] J. Qiu, J. Ma, W. Han, X. Wang, M. Heini, B. Li, D. Sun, R. Zhang, Y. Shi. Polymers, **15**, 3805 (2023). DOI: 10.3390/polym15183805
[4] A. Oshima, F. Shiraki, H. Fujita, M. Washio. Rad. Phys. Chem., **80**, 196 (2011). DOI: 10.1016/j.radphyschem.2010.07.032
[5] N.I. Cherkashina, V.I. Pavlenko, M.M. Mikhailov, A.N. Lapin, S.A. Yuriev, N.I. Bondarenko. Acta Astronautica, **193**, 209 (2022). DOI: 10.1016/j.actaastro.2021.12.034
[6] N.I. Cherkashina, V.I. Pavlenko, A.V. Noskov, D.S. Romanyuk, R.V. Sidelnikov, N.V. Kashibadze. Adv. Space Res., **70**, 3249 (2022). DOI: 10.1016/j.asr.2022.07.051
[7] A. Rahnamoun, D.P. Engelhart, S. Humagain, H. Koerner, E. Plis, W.J. Kennedy. Polymer, **176**, 135 (2019). DOI: 10.1016/j.polymer.2019.05.035
[8] T. Paulmier, B. Dirassen, M. Arnaout, D. Payan, N. Balcon. IEEE Trans. Plasma Sci., **43**, 2907 (2015). DOI: 10.1109/TPS.2015.2452943
[9] M.I. Gurevich, E.D. Kazakov, Yu.G. Kalinin, A.A. Kurilo, O.V. Tel'kovskaya, K.V. Chukbar. Tech. Phys., **91**, 2194 (2021). DOI: 10.21883/TP.2022.14.55218.346-20
[10] P.B. Sergeev, N.V. Morozov. Opt. Spectr., **126** (2019). DOI: 10.1134/S0030400X19030214
[11] D. Drouin, A.R. Couture, D. Joly, X. Tastet, V. Aimez, R. Gauvin. Scanning, **29**, 92 (2007). DOI: 10.1002/sca.20000
[12] P. Hovington, D. Drouin, R. Gauvin. Scanning, **19**, 1 (1997). DOI: 10.1002/sca.4950190101
[13] E.M. Höppener, M. Shahmohammadi, L.A. Parker, S. Henke, J.H. Urbanus. Talanta, **253**, 123985 (2023). DOI: 10.1016/j.talanta.2022.123985
[14] G. Demol, T. Paulmier, D. Payan. IEEE Trans. Plasma Sci., **51** (9), 2584 (2023). DOI: 10.1109/TPS.2023.3269583
[15] V.I. Oleshko, E.Kh. Baksht, A.G. Burachenko, V.F. Tarasenko. Tech. Phys., **62**, 299 (2017). DOI: 10.1134/S1063784217020232
[16] J. Mihaly, S. Sterkel, H. Ortner, L. Kocsis, L. Hajba, É. Furdyg. Croat. Chem. Acta, **79**, 497 (2006).
[17] E. Plis, D.P. Engelhart, D. Barton, R. Cooper, D. Ferguson, R. Hoffmann. PSS (b), **254** 1600819 (2017). DOI: 10.1002/pssb.201600819
[18] H. Ishida, S.T. Wellinghoff, E. Baer, J.L. Koenig. Macromolecules, **13**, 826 (1980). DOI: 10.1021/ma60076a011
[19] G. Jinglong, N. Zaochun, L. Yanhui. E-Polymers, **16**, 111 (2016). DOI: 10.1515/epoly-2015-0223

Translated by D.Safin